J. PHYS. IV FRANCE 7 (1997)
Colloque C5, Supplément au Journal de Physique III de novembre 1997

Generation of Recovery Stresses: Thermodynamic Modelling and Experimental Verification

R. Stalmans, L. Delaey and J. van Humbeeck

Department of Metallurgy and Materials Engineering, K.U. Leuven, de Croylaan 2, 3001 Heverlee, Belgium

Abstract: Shape memory elements generate significant recovery stresses when the shape recovery associated with the reverse martensitic transformation is impeded during heating. This process of stress generation is influenced by many parameters. A fundamental model has been developed to describe this generation of recovery stresses. The model is based on a generalised thermodynamic analysis of shape memory behaviour. The mathematical approach and the assumptions in this model are selected in such a way that the calculations yield close approximations of the real behaviour and that the final mathematical equations are relatively simple. The paper presents also experimental measurements of recovery stress generation for complex restraining conditions. Comparison of the experimental results with the calculated results confirm that this model can be used to predict quantitatively the generation of recovery stresses.

1. INTRODUCTION

Recovery forces are generated when the shape recovery during heating, i.e. the one way memory effect, is impeded. The processes can be summarised as follows. Prestrained, martensitic SMA-elements operate during heating against mechanical obstacles, such as the bias spring and the bias force in fig.1. Since the shape recovery of the SMA-elements, associated with the reverse transformation during heating, is hampered, high recovery forces are generated gradually by the SMA-elements (and shape recovery of the SMA-elements is delayed). Vice versa, the recovery forces decrease during cooling after overcoming a temperature hysteresis (and the SMA-elements become strained).

This process of stress generation and strain recovery corresponds to a complex, non-linear thermomechanical behaviour with hysteresis. Moreover, this complex behaviour is influenced by a large number of parameters. It follows that there are in general no direct and simple relations between the temperature, the position (or strain) and force (or stress). This emphasises the need for comprehensive constitutive models that can accurately describe the thermomechanical behaviour and have moreover a mathematical expression in a form that is amenable to incorporation into other engineering tools. A recently developed model based on a generalised thermodynamic analysis of the underlying martensitic transformation is presented in this paper in §3.

Accurate experimental data on this process of stress generation for complex strain conditions are lacking in open literature. Therefore, experimental results are first presented in §2. Experimental results and calculated results are compared in §4.

2. EXPERIMENTAL DATA ON THE GENERATION OF RECOVERY STRESSES

Some input parameters in the modelling have to be determined by experiments. Also, the accuracy of the modelling has to be verified and optimised by comparison with experimental results. For these purposes, series of experiments have been performed on a fully computerised apparatus [1] which offers the possibilities for complex coupled control of stress, strain and temperature . The results obtained on Ni-Ti-6wt%Cu wires with a diameter of 1.15 mm are shown in fig.2 and fig.3. The samples have been aged for 20' at 823K, and underwent afterwards a training treatment (100 thermomechanical cycles) to obtain a stable shape memory behaviour.

Figure 2.b shows a strain-temperature curve during free recovery. The sample was (i) heated to 353 K, which is above A_f, (ii) loaded with a stress equal to 235 MPa, (iii) cooled to 303 K, which is below M_f, (iv) unloaded and (v) heated to 363 K. The strain-temperature curve during the latter heating is shown on the figure.

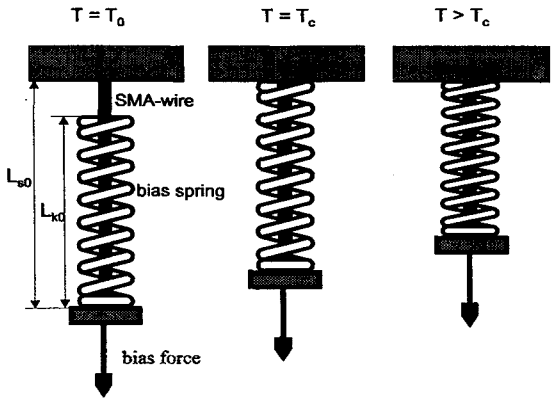

Figure 1: Schematic drawing of the example system. The strain recovery of the SMA-wire is hampered by a constant force F_C and a linear spring with spring constant k.

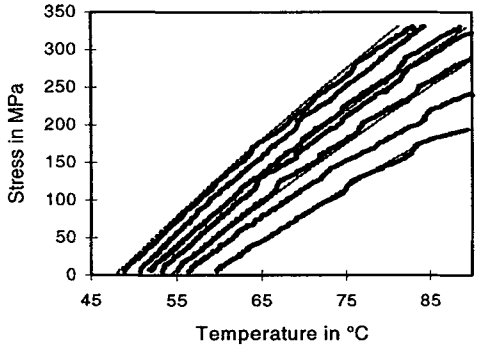

Figure 2.a: Stress-temperature curves, showing the generation of recovery stresses. During heating from the martensitic state free recovery was allowed until a programmed contact strain e_C was obtained. During further heating the strain was controlled as a linear function of the temperature, as shown in 2.b. Results calculated with the modelling are given in dashed lines for the following values of e_C (in %): 1.90, 1.60, 0.75 and 0.30.

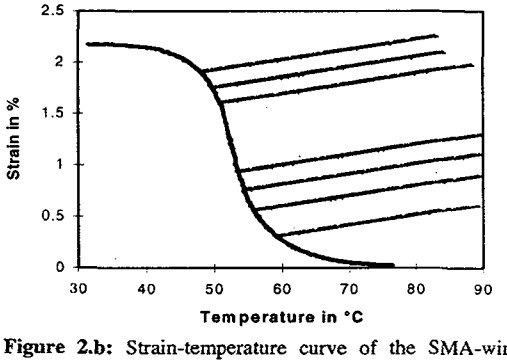

Figure 2.b: Strain-temperature curve of the SMA-wire during free recovery and the strain paths imposed during the experiments of which the generated stresses are shown in fig.2.a. The simulated thermal dilatation coefficient was in all experiments equal to $100*10^{-6}$/K.

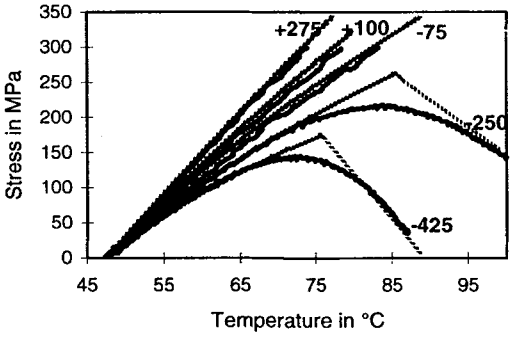

Figure 3.a: Stress-temperature curves, showing the generation of recovery stresses. During heating from the martensitic state free recovery was allowed until a programmed contact strain e_C was obtained. The contact strain was in all experiments equal to 1.9%. During further heating the strain was controlled as a linear function of the temperature, as shown in fig.3.b. The simulated thermal dilatation coefficients (in $100*10^{-6}$/K) are indicated above the curves. Results calculated with the modelling are given in dashed lines.

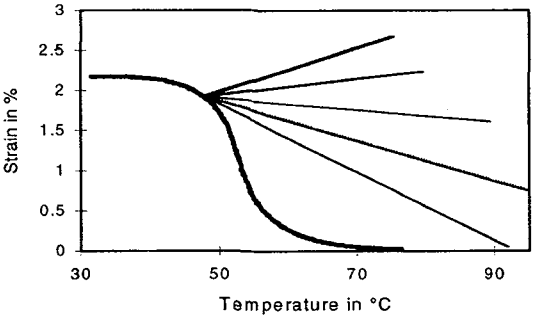

Figure 3.b: Strain paths imposed during the experiments of which the generated stresses are shown in fig.3.a.

Figure 2.a and fig.3.a show the generation of recovery stresses. In these experiments, steps (i) to (iv) are identical to the experimental procedure above. In step (v) free recovery was allowed until a programmed contact strain e_c was obtained. During further heating the strain e was controlled in the following way, with T the temperature and α a parameter:

$$e = e_c + \alpha * \Delta T \quad |1|$$

Figure 2.a and fig.3.a show the results for different values of respectively e_c and α.

3. CONSTITUTIVE MODELLING OF THE GENERATION OF RECOVERY STRESSES

The functional properties of shape memory alloys, including the ability to generate recovery forces, are closely linked to a crystallographically reversible, thermoelastic martensitic transformation [2, 3]. A generalised thermodynamic model of this thermoelastic transformation has been developed in order to predict the thermomechanical behaviour of shape memory elements [4-7]. The use of this thermodynamic model has already resulted in an increased fundamental understanding of shape memory behaviour, and especially of the relationships between training, the two way memory effect, and related effects [4-6]. As an example of quantitative calculations and of the practical applicability, it is shown here that this fundamental modelling can be applied in the design of engineering systems where the generation of recovery force is the utilised functional property.

The general procedures are illustrated by the example of the system depicted in fig.1. Applying the same principles, equations for more complex systems can be easily developed. There are two mechanical components hampering the strain recovery of the SMA-wire in fig.1. The first component is a constant bias force F_c. The second component is a bias spring with spring constant k and thermal dilatation coefficient α. A completely rigid system can be modelled by taking the spring constant equal to infinity. The SMA-wire has a predeformation equal to e_{s0} at the start temperature T_0, which is below M_f. Four temperature regions can be distinguished during heating of this system, starting from T_0.

1. The SMA-wire is in the martensitic state between T_0 and $A_s(\sigma_c)$, the temperature at which the reverse martensitic transformation and the concomitant shape recovery start; σ_c is given by F_c divided by the cross section Q of the SMA-wire.
2. The reverse martensitic transformation and the shape recovery proceed against the bias force F_c until contact is made with the bias spring at a temperature T_c.
3. From the temperature T_c, the retransformation and the shape recovery is restrained by the bias spring and the constant bias force. The retransformation gradually proceeds until a temperature T_{se}, the temperature at which the retransformation ends.
4. Above T_{se}, the SMA-wire is in the parent state ('austenite').

The total strain of the SMA-wire, indicated by e_s, can always be divided into a recoverable shape memory strain e_{sr}, a thermal dilatation e_{sa} and an elastic strain e_{se}:

$$e_s = e_{sr} + e_{sa} + e_{se} = e_{sr} + \alpha_s * (T - T_0) + \sigma_s / E_s \quad |2|$$

with T the temperature and σ_s, α_s and E_s respectively stress on the SMA-wire, thermal dilatation coefficient and elasticity modulus of the SMA-wire.
The force exerted by the bias spring is given by:

$$F_k = k * (L_k - L_{k0} * (1 + \alpha * (T - T_0)) \quad |3|$$

with L_k the length of the bias spring at temperature T, L_{k0} the length of the spring at the start temperature T_0, and k the bias spring constant.

In the thermodynamic modelling, mentioned in the introduction, global and local thermodynamic equilibrium conditions have been deduced. Details can be found in [4, 6]. Differentiation of the global equilibrium condition yields a generalised Clausius-Clapeyron equation:

$$\{d\sigma_s/dT\}_{[\xi]=cst} = -(\rho_0 * \Delta s)/\Delta e_{tr\Sigma A}([\xi]) \quad |4|$$

The parameters in the right-hand part have a clear physical meaning. Δs is the entropy change during transformation from austenite to martensite. ρ_0 is the mass density of the SMA-wire in stress-free conditions. $\Delta e_{tr\Sigma A}([\xi])$ represents the average transformation strain on all austenite-martensite interfaces corresponding with a transformation fraction $[\xi]$. An important remark is that the transformation strain, $\Delta e_{tr\Sigma A}([\xi])$, is a complex function of $[\xi]$ and is also influenced by the heat treatment, the processing parameters and the thermomechanical history [4, 5]. Moreover, the direct determination of the complex function $\Delta e_{tr\Sigma A}([\xi])$ is very difficult and thus inefficient for practical applications. However, for a given

alloy, thermomechanical treatment, and predeformation e_{s0}, the stress rate $\{d\sigma_s/dT\}_{[\xi]=cst}$ can be approximated as a function of e_{sr}:

$$\{d\sigma_s/dT\}_{[\xi]=cst} = f_{cc}([\xi]) \approx f_{cc}(e_{sr}) \quad |5|$$

with f_{cc} an abbreviation of $\{-(\rho_0*\Delta s)/\Delta e_{tr\Sigma A}\}$.
The function $f_{cc}(e_{sr})$ can be accurately determined from a minimum of experiments as explained in §4.

3.1 The temperature region from T_0 to A_s

The SMA-wire is in the martensitic state between T_0 and $A_s(\sigma_c)$. It follows immediately that in the first temperature region the thermomechanical behaviour is described by:

$$e_s = e_{s0} + (F_c/Q*E_s) - \alpha_s*T_0 + \alpha_s*T \quad |6|$$

with e_{s0} the recoverable deformation of the SMA-wires at zero stress at the starting temperature T_0

The start temperature of the reverse transformation $A_s(\sigma_c)$ is influenced by the constant external stress σ_c. From integration of |4| follows directly:

$$A_s(\sigma_c) = A_s(0) + \sigma_c*f_{cc}(e_{s0}) \quad |7|$$

3.2 The temperature region from A_s to T_c

In the second temperature region from $A_s(\sigma_c)$ to T_c, the shape recovery proceeds against the bias force F_c until contact is made with the bias spring at T_c. Since σ_s is given by $\{F_c/Q\}$, |2| can be simplified to the following boundary condition:

$$e_s = (F_c/Q*E_s) - \alpha_s*T_0 + e_{sr} + \alpha_s*T \quad |8|$$

The right-hand part of this boundary condition holds the unknown e_{sr}. The reverse transformation proceeds during further heating, i.e. e_{sr} decreases. From integration of |4| follows a relationship between the temperature T and e_{sr}:

$$T(e_{sr}, \sigma_c) = T_{tr}(e_{sr}, 0) + \sigma_c*f_{cc}(e_{sr}) \quad |9|$$

with $T_{tr}(e_{sr}, 0)$ the transformation temperature corresponding with e_{sr} when the stress is equal to zero.

Contact with the bias spring is made at the temperature T_c. The mathematical equivalent is:

$$e_s = (L_s - L_{s0})/L_{s0} \geq (L_{k0} - L_{s0} - L_{k0}*\alpha*T_0 - F_c/k)/L_{s0} + (L_{k0}*\alpha/L_{s0})*T + \sigma_s*Q/(k*L_{s0}) \quad |10|$$

The strain e_s becomes equal to the right-hand part of |10| at T_c.

3.3 The temperature region from T_c to T_{se}

In the third temperature region, the derivation is more complicated. The strain recovery of the SMA-wire is hampered by the constant bias force and the bias spring. A mathematical formulation of this boundary condition follows directly from the equations that express stress and strain equilibrium. This equilibrium implies an equal sign in equation |10|. This general boundary equation corresponds to a plane in the thermomechanical $\{e_s\text{-}T\text{-}\sigma_s\}$-space, and can be simplified to:

$$e_s = C_1 + C_2*T + C_3*\sigma_s \quad |11|$$

in which C_1, C_2 and C_3 are three system constants given by:

$$C_1 = \{(L_{k0} - L_{k0}*\alpha*T_0 - F_c/k)/L_{s0}\}, \quad C_2 = \{\alpha*L_{k0}/L_{s0}\} \quad \text{and} \quad C_3 = \{Q/(k*L_{s0})\} \quad |11'|$$

An extra equation is required in order to solve e_s and σ_s as a function of the temperature. From the derivations follows that the Clausius-Clapeyron equation (|4|) is only valid for conditions of constant $[\xi]$ or the equivalent, for constant e_{sr}. A modified Clausius-Clapeyron equation that is valid for the situation of non-constant $[\xi]$ in the third temperature region can be derived on the basis of the Clausius-Clapeyron equation, as illustrated in fig.4. The starting point corresponds to a recovery stress equal to σ_s at a temperature T and a strain e_s. An infinitesimal temperature increase dT induces a stress increase $d\sigma_s$ and a strain change de_s. This infinitesimal step from A (T, σ_s, e_s) to C (T+dT, σ_s+$d\sigma_s$, e_s+de_s) can be also achieved in two intermediate steps.
The first step (A→B) is an infinitesimal temperature increase dT *at constant transformation fraction [ξ] and thus at constant e_{sr}*. This temperature increase yields an increase of the stress by $d\sigma_r$. The stress increase $d\sigma_r$ is given directly by |4|. The resulting increases of the elastic strain de_e and of the thermal dilatation follow directly from |2|.

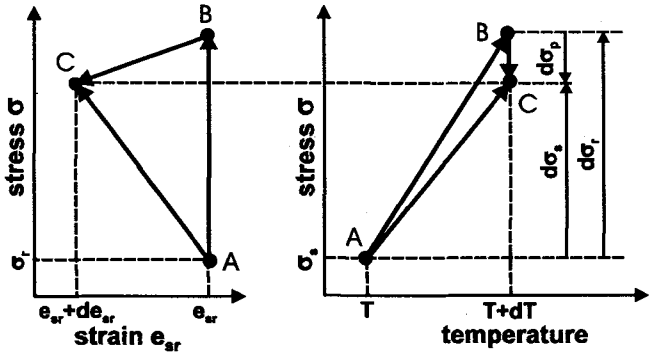

Figure 4: The process of a temperature increase dT at the imposed boundary conditions (A→C) can be replaced by a temperature increase at a constant transformation strain (A→B), followed by an unloading at constant temperature (B→C).

The second step (B→C) is unloading by $d\sigma_p$ *at constant temperature {T+dT}*. This unloading results in a pseudoelastic decrease of the strain by de_p, approximated by:

$$de_p = d\sigma_p / P_s \qquad |12|$$

with P_s the pseudoelastic modulus, given by the slope $d\sigma_s/de_s$ during pseudoelastic unloading.
It follows that the stress increase $d\sigma_s$, respectively strain change de_s, are given by:

$$d\sigma_s = d\sigma_r + d\sigma_p \qquad \text{and} \qquad de_s = de_e + de_a + de_p \qquad |13|$$

Combination of equations |11-13| results finally in the differential constitutive equation which is valid *during retransformation* in the temperature region $\{T_c \rightarrow T_{se}\}$:

$$d\sigma_s/dT = P_s*(C_2 - \alpha_s)/(1 - P_s*C_3) + f_{cc}(e_{sr})* \{1 - (P_s/E_s)\}/(1 - P_s*C_3) \qquad |14|$$

The shape memory strain e_{sr} decreases gradually. The end temperature T_{se} follows from the condition that e_{sr} becomes equal to zero.

3.4 The temperature region above T_{se}

In the fourth temperature region the SMA-wire is in the parent state. It follows immediately from |2| and |11| that in this temperature region the stress σ_s is given by:

$$\sigma_s = E_s*\{C_1 + \alpha_s*T_0 + C_2*T - \alpha_s*T\}/(1 - E_s*C_3) \qquad |15|$$

4. APPLICATION AND EVALUATION OF THE MODELLING

Only a limited set of easy-to-determine input data are required to solve the above set of equations.
First, a free recovery curve, as in fig.2.b, allows to determine $T_{tr}(e_{s0}, 0)$ required in |9|.
Second, it has been shown [4] that $f_{cc}(e_{sr})$ can be closely approximated by a linear function:

$$f_{cc}(e_{sr}) \approx S_1*e_{sr} + S_2 \qquad |16|$$

The measurement of the slopes $\{d\sigma_s/dT\}$ near to T_c for a low and a high value of e_c allows to determine the material parameters S_1 and S_2. The two extreme curves in fig.2.a have been used for this purpose. Third, the elastic modulus E_s and pseudoelastic modulus P_s are calculated from a linear approximation of the slope $d\sigma/de$ during respectively elastic and pseudoelastic loading. A last material parameter is the thermal dilatation coefficient α_s.

The system is characterised by the following set of input variables: the cross section of the SMA-wire Q, the bias force F_c, the bias spring constant k, the starting temperature T_0, the initial deformation e_{s0} of the SMA-wires, the lengths L_{k0} and L_{s0}, and the thermal dilatation coefficient α.

For such sets of input variables, the stress σ_s and strain e_s during heating can be easily computed from the equations above. A simple computer program 'SMA-hybrid' has been developed for this purpose. Calculated results are shown in fig. 2.a and fig.3.a by dashed lines. A comparison of the computed results with the experimental results shows an accurate *quantitative* agreement. Quantitative agreement between calculated results and experimental results has also already been shown for different boundary conditions on Cu-base SMA-wires [5]. This excellent quantitative agreement for an extremely wide range of the parameters e_c and α is also a confirmation of the general validity of the applied thermodynamic equations.

It can be easily shown that the factor $\{1 - (P_s/E_s)\}/(1- P_s*C_3)$ in the second term of |14| is in general close to 1. Typical values of $f_{cc}(e_{sr})$ are 3 to 20 MPa/K. It can be also shown that the absolute value of the first term $\{P_s*(C_2 - \alpha_s)/(1- P_s*C_3)\}$ in |14| is in general smaller than 0.2 MPa/K. This indicates that the stress rate $\{d\sigma_s/dT\}$ in |14| is mainly determined by the 'Clausius-Clapeyron' term and only to a very small extent by the system parameters, as confirmed in fig.3. Figure 3 shows clearly that the slopes $\{d\sigma_s/dT\}$ at the start of the third temperature region (48°C) are hardly influenced by large changes of the system parameter α.

The stress rate $\{d\sigma_s/dT\}$ after retransformation can be obtained by differentiation of |15|:

$$d\sigma_s/dT = E_s*\{C_2 - \alpha_s\}/(1 - E_s*C_3) \qquad |17|$$

In a first approximation it follows from a comparison of |14| with |17| that changes of the stress rate $\{d\sigma_s/dT\}$ as a result of changes of the input variables are proportional to P_s during retransformation and proportional to E_s after retransformation. Since P_s is much smaller than E_s, it follows that the system input variables (Q, k, L_{k0}, L_{s0} and α) have a much smaller influence on the stress rate $\{d\sigma_s/dT\}$ during retransformation than after retransformation, as can be easily seen from a comparison of these two temperature regions in the curves for α equal to $-250*10^{-6}$/K and $-425*10^{-6}$/K in fig.3. This simple but important difference between |14| and |17| is however not taken into account in many other models.

5. CONCLUSIONS AND FURTHER DEVELOPMENTS

In this paper a general thermodynamic modelling has been applied for the prediction of recovery stresses in complex restraining conditions. Experimental verification has confirmed that these thermodynamic equations can yield accurate results for engineering cases. The simplicity of the mathematical equations implies also that this scheme of calculations can be used for the study of very complex cases, including finite element calculations. Moreover, the calculations only require a limited number of simple to determine shape memory data.

Since the final mathematical equations are relatively simple, this type of modelling can be also used by users without any knowledge of the thermodynamic background. On the other hand, due to the clear physical meaning of the parameters and the large area of application, this type of modelling can also contribute to a better understanding of different fundamental aspects of shape memory behaviour.

The modelling and computer programs are further developed and improved. One of the major aims is the development to an effective tool for the materials design of matrix materials with embedded SMA-wires. In the current approach constant values were used for the parameters α_s, E_s, and P_s and the function $f_{cc}(e_{sr})$ was approximated as a linear function of e_{sr}. The effect of applying more complex algorithms will be investigated in near future. Another development is the inclusion of irreversible thermodynamic contributions to describe the influence of hysteresis on the thermomechanical behaviour of shape memory alloys.

Acknowledgements

R. Stalmans and J. Van Humbeeck acknowledge the F.W.O. Vlaanderen for a grant as Postdoctoral Fellow, respectively Research Leader.

References

[1] Stalmans R., Van Humbeeck J. and Delaey L., *Acta metall. mater.* **40** (1992) 501-511.
[2] Delaey L., "Diffusionless Transformations", in: Materials science and technology, Vol.5, Phase transformations in materials, P. Haasen Ed. (VCH Verlagsgesellschaft mbH, Weinheim, Germany, 1991) pp. 339-404.
[3] Ahlers M., *Progress in materials science* **30** (1986) 135-186.
[4] Stalmans R., Shape memory behaviour of Cu-base alloys, Doctorate Thesis (Catholic University of Leuven, Department of Metallurgy and Materials Science, Heverlee, Belgium, 1993).
[5] Stalmans R., Van Humbeeck J. and Delaey L., *Journal de physique IV - Colloque C8* **5** (1995) 203-207.
[6] Stalmans R., Van Humbeeck J. and Delaey L., "A generalized thermodynamic model to predict shape memory behaviour", AMD-Vol189/PVPVol.292: Mechanics of phase transformations and shape memory alloys - ASME 1994, C. Brinson and B. Moran Eds. (ASME, Chicago, USA, 1994) pp. 39-44.
[7] Stalmans R., Van Humbeeck J. and Delaey L., "Modelling of adaptive composite materials with embedded shape memory alloy wires", Mat. Res. Soc. Symp. Proc. Vol 459: Materials for smart systems II, E. P. George, R. Gotthardt, K. Otsuka, S. Trolier-McKinstry and M. Wun-Fogle Eds (Materials Research Society, Pittsburgh, USA, 1997) pp. 119-130.